



Defected ground structure band-stop filter by semicomplementary split ring resonators

M. Naghshvarian-Jahromi M. Tayarani

Department of Electrical Engineering, Iran University of Science and Technology (IUST), Tehran, Narmak, Iran
 E-mail: 82412117@ee.iust.ac.ir; m.naghshvarian@ee.iust.ac.ir

Abstract: This study proposes a band-stop filter using a defected ground structure. The notch frequency is produced by an array of two semicomplementary split ring resonators (SCSRRs), etched on the ground plane and two line resonators etched out of the microstrip line. Band reject behaviour is exhibited due to the presence of a negative effective dielectric permittivity near the resonance frequency. The filter produces high rejection with sharp cutoffs in the stop band, and shows a completely flat and lossless passband. In addition, because of the geometrical structure of the resonators and the filter, even harmonics responses of the filter are eliminated. The proposed filter is constructed on a substrate with a thickness of 0.8128 mm, ϵ_r of 3.55 and dimensions of $30 \times 45 \text{ mm}^2$. Measurements show an insertion loss below 30 dB from 2.3 to 2.7 GHz and a maximum insertion loss of 44 dB at around 2.53 GHz. The electrical size of the filter is small due to the sublambda operation of SCSRRs and is verified in the last section by comparing the proposed filter with other familiar metamaterials such as complementary split ring resonator. Moreover, the distributed equivalent circuit model based on geometrical filter parameters is introduced.

1 Introduction

In recent years, one of the burning issues in the RF, microwave and millimetre-wave systems community has been the design of filters with high rejection and sharp cutoffs in the stop band. Making a completely flat and lossless pass-band filter is an important challenge to conventional microwave systems and microwave circuit design methodologies. Nowadays, most band-stop filters in the RF, microwave and millimetre-wave frequencies are found in waveguides, printed circuit boards, defected ground structure (DGS) and other media [1, 2]. Extensive, a thorough research to develop novel metamaterials and their utilisation in microwave devices is underway. Electromagnetic (EM) band-gap structures, negative- ϵ , negative- μ and left-handed media are the most popular metamaterials that are used in the microwave and millimetre-wave community [3–12]. However, the optimisation process for microwave structures using full-wave commercial software is a time-consuming task. Thus, to resolve this problem, lumped-element models including an LC-network resonator and a distributed model using transmission lines have been reported [13–18].

Here we introduce a new semicomplementary split ring resonator (SCSRR) and propose an improved model for these resonators. The model is verified by the good agreement between EM simulations, circuit simulations and measured results within a very wide frequency range. Furthermore, a band-stop filter using SCSRRs in the ground plane and two line resonators (LRs) in the microstrip line is fabricated and measured to demonstrate the predicted results. The measurement shows an insertion loss below

30 dB from 2.3 to 2.7 GHz and a maximum insertion loss of 44 dB at around 2.53 GHz. Section 6 provides a comparison of the results for this proposed filter with other familiar metamaterials such as complementary split ring resonator as reported in [19].

2 Proposed filter design

The schematic view and the dimensions of the SCSRR filter are shown in Fig. 1. Rogers RO4003 with a thickness of 0.8128 mm (32-mil) and a relative dielectric constant of 3.55 is used as the substrate in simulations and measurements. The other parameters are shown in Fig. 1c, and the LR parameters are as follows $W_1 = 0.4 \text{ mm}$, $W_2 = 0.3 \text{ mm}$, $W_3 = 1.7 \text{ mm}$, $S_1 = 0.3 \text{ mm}$ and $S_2 = 0.9 \text{ mm}$. In addition, the other SCSRR parameters are $W_{os} = 0.2 \text{ mm}$ and $W_{sq} = 3.0 \text{ mm}$. The fabricated filter is shown in Fig. 2. Fig. 2a shows the top view of the proposed filter and Fig. 2b shows the bottom view.

3 Band-stop filter design using SCSRRs

Fig. 3 shows the physical configuration of a unit cell of the novel SCSRR structures. First, the scattering parameters are obtained by a full-wave simulator and the results are shown in Fig. 4 (note the reference planes for S-parameters are shown in Fig. 3 and the SCSRR (in Fig. 3) has same dimension such as the proposed filter in Fig. 1). Next, the electric permittivity and the magnetic permeability of the transmission line are computed. The scattering parameters illustrate that a band-stop

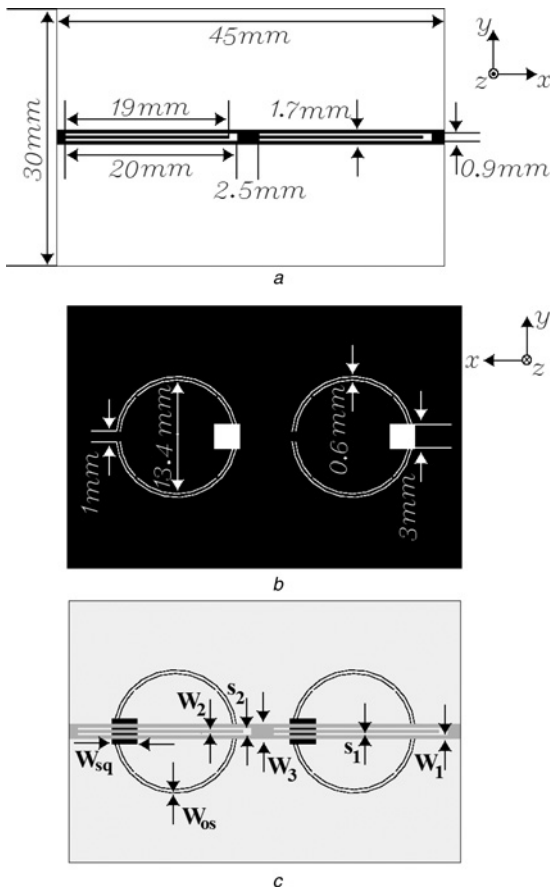


Fig. 1 Schematic diagram of the SCSRR band-stop filter with geometrical dimensions

- a Top view of the filter with LRs
- b Bottom view with the SCSRR-shaped DGS
- c Top and transparent bottom views of the proposed filter

characteristic is present at a resonant frequency of 2.5 GHz where the rejection level reaches about 35 dB.

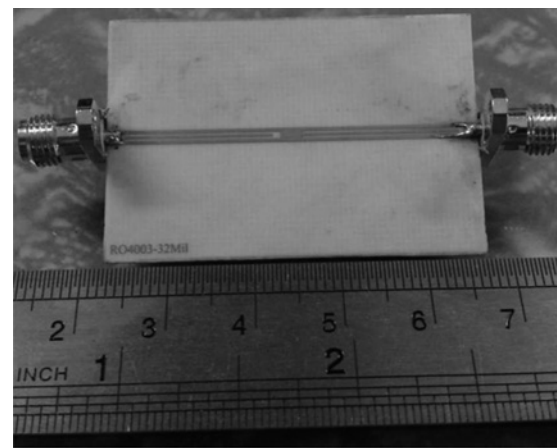
The effective medium theory on an inhomogeneous left-handed media can be substituted by an equivalent homogeneous media with effective permeability μ_{eff} and permittivity ϵ_{eff} such that the macroscopic (i.e. the wavelength is big enough when compared with the dimensions of the basic scattering elements that create the left-handed medium) properties of the equivalent media are the same as the original non-homogeneous media. An efficiently homogeneous structure with average unit cell size (about 14.0 mm) is much smaller than the guided wavelength λ_g (in notch frequency). Thus, this average cell size should be at least smaller than a quarter wavelength, $l < \lambda_g/4$. Hence, this condition guarantees that when a wave propagates inside the metamaterial medium, the unit cell behaves as a lumped element circuit. The following equations take out the μ_{eff} and the ϵ_{eff} [20–23]

$$\Gamma = k \pm \sqrt{k^2 - 1} \quad (1)$$

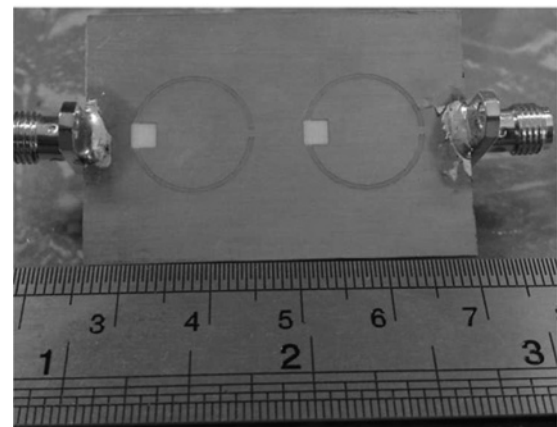
where the sign of \pm is determined by $|\Gamma| \leq 1$ and

$$k = \frac{S_{11}^2 - S_{21}^2 + 1}{2S_{11}}$$

$$z_{\text{eff}} = \sqrt{\frac{\mu_{\text{eff}}}{\epsilon_{\text{eff}}}} = \left(\frac{1 + \Gamma}{1 - \Gamma} \right) \frac{Z_a^{\text{TL}}}{Z_b^{\text{TL}}} \quad (2)$$



a



b

Fig. 2 Fabricated SCSRR band-stop filter

- a Top view
- b Bottom view

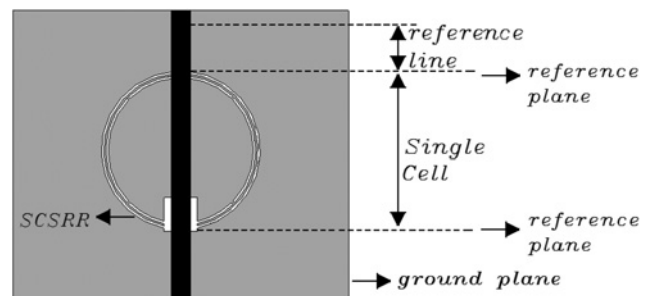


Fig. 3 Single-cell SCSRR structure

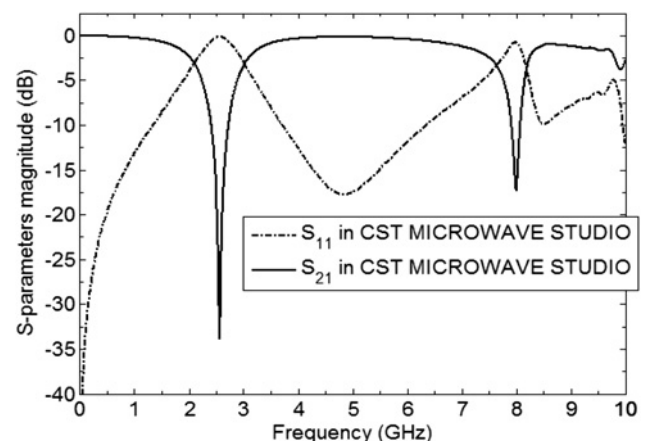


Fig. 4 S-parameters for single-cell SCSRR

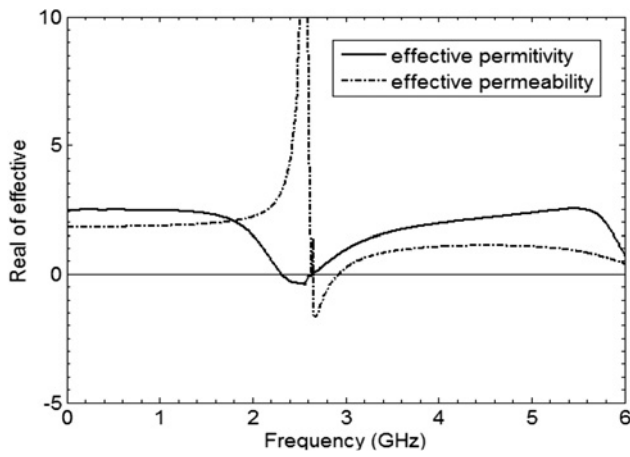


Fig. 5 Extracted real effective permittivity and permeability for a one-unit SCSRR

$$n = n' - jn'' = \sqrt{\epsilon_{\text{eff}} \mu_{\text{eff}}}$$

$$= \pm \frac{c}{j\omega l} \cosh^{-1} \left(\frac{1 - S_{11}^2 + S_{21}^2}{2S_{21}} \right) \quad (3)$$

$$\epsilon_{\text{eff}} = \epsilon'_{\text{eff}} - j\epsilon''_{\text{eff}} = \frac{n}{z_{\text{eff}}} \quad (4)$$

$$\mu_{\text{eff}} = \mu'_{\text{eff}} - j\mu''_{\text{eff}} = n \cdot z_{\text{eff}} \quad (5)$$

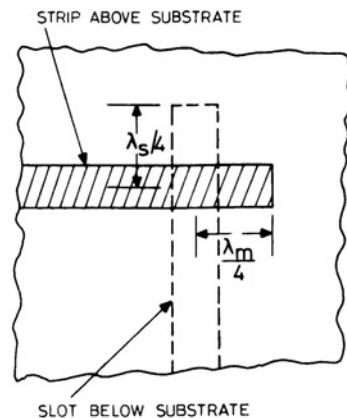
where Z^{TL} and Z_a^{TL} are the characteristic impedances of the

reference transmission line and the air-filled reference transmission line, respectively, and n is the effective refractive index of the medium. If the material is passive, the requirement of causality ($\text{Im}(n) < 0$) fixes the choice of sign in (3) [24].

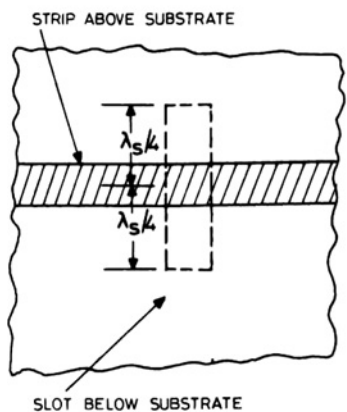
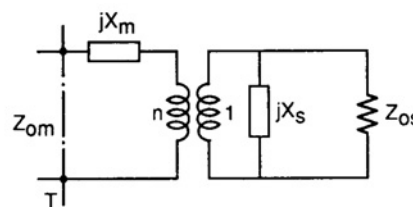
Frequency dependencies of the simulated effective parameters of the SCSRR structure are shown in Fig. 5. Examining the extracted ϵ_{eff} and μ_{eff} shows the reason for the band-stop characteristic, and it is due to the presence of negative ϵ_{eff} at high positive μ_{eff} resonance. A negative μ_{eff} is seen at small positive ϵ_{eff} . It is well known that materials, which exhibit either negative ϵ_{eff} or negative μ_{eff} , do not allow any wave propagation. This can be proved by analysing the refractive index relation $n = \pm \sqrt{\epsilon_{\text{eff}} \mu_{\text{eff}}}$. If both the ϵ_{eff} and the μ_{eff} are negative simultaneously, then a left-handed wave propagation is permitted. It is important to note that the negative ϵ_{eff} response is for a unit cell only and is shown to demonstrate the existence of a negative ϵ_{eff} property of the SCSRR. For an array of SCSRRs in one or two dimensions, the effective permittivity cannot be extracted using this method as increasing the number of unit cells will exceed the effective homogeneity limit [25].

4 Extracting distributed equivalent circuit model

By means of this concept, an SCSRR can be etched as a ring in the ground plane, just underneath the microstrip line. This arrangement leads to the proper excitation of the SCSRR by the magnetic field. It is important to note that the



a



b

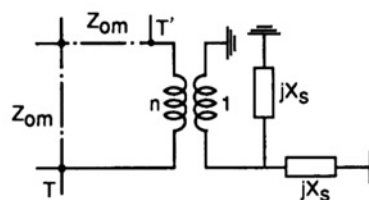


Fig. 6 Equivalent lumped model for coupling the microstrip line to the slot line

a Picture from [26]

b Supplement for use in the filter equivalent circuit

so-obtained SCSRR is not rigorously the dual of the conventional SRR. In addition, LRs are designed as a $\lambda_g/4$ (at the centre frequency) resonator inserted in the main microstrip transmission line, and this leads to a reduction in the size of the filter. These lines magnetically couple to the SCSRR at the rejection band. For modelling the proposed filter, the fact that the slot line is the complementary of microstrip line was useful. In addition, for the coupling of the microstrip line to the slot, the concept described in [27] and shown in Fig. 5a was used. Fig. 6a was supplemented in Fig. 6b for use in the equivalent circuit. The circumference of the SCSRR is about $\lambda_g/2$ and the turn ratio can be calculated by $n = \sqrt{Z_{om}/Z_{os}}$ [17, 18]. In addition, the formulas presented in [27] were used for calculating the characteristic impedance and the effective permittivity of the slot lines and at $f_0 = 2.5$ GHz. These are equal to 83.2 Ω and 1.6 for W_{os} and 148.5 Ω and 1.23 for W_{sq} , respectively.

The proposed equivalent circuit model is shown in Fig. 6. Some other required values for Fig. 7 are listed in Table 1, and this model is simulated with the AWR Design Environment [18]. The results are shown in Fig. 8 from 0.5 to 10 GHz and compared with the CST Microwave Studio [28] EM simulation results. There is good agreement between full-wave simulation and the proposed model results. All parameters of this model have physical dimensions or can be calculated by physical parameters such as characteristic impedance and effective permittivity for slot lines.

Table 1 Some required values required for the equivalent circuit model in Fig. 7 at 2.5 GHz

Type	Value
Z_{om1}	104.5 Ω
Z_{om2}	115.2 Ω
Z_{os}	83.2 Ω
Z_{sq}	148.5 Ω
N_1	$\sqrt{Z_{om1}/Z_{sq}}$
N_2	$\sqrt{Z_{om2}/Z_{sq}}$

5 Design methodology

To design a band-reject filter of the proposed form at f_0 (the centre frequency), the larger circumference of the SCSRR is chosen around $\lambda_g/2$ at f_0 . Then, the coupling coefficient is decided by the width of W_{sq} for the desired rejection level. This entails changing the effective permittivity and the characteristic impedance after changing the n_1 and the n_2 in the equivalent circuit. Next, the second SCSRR is added to the structure to achieve the desired bandwidth, and now the proposed structure has two resonances in the rejection band. For widening the rejection bandwidth, the $\lambda_g/2$ (at f_0) LRs are added in the main line. A double pole and therefore a deep rejection are added to the response. The upper and the

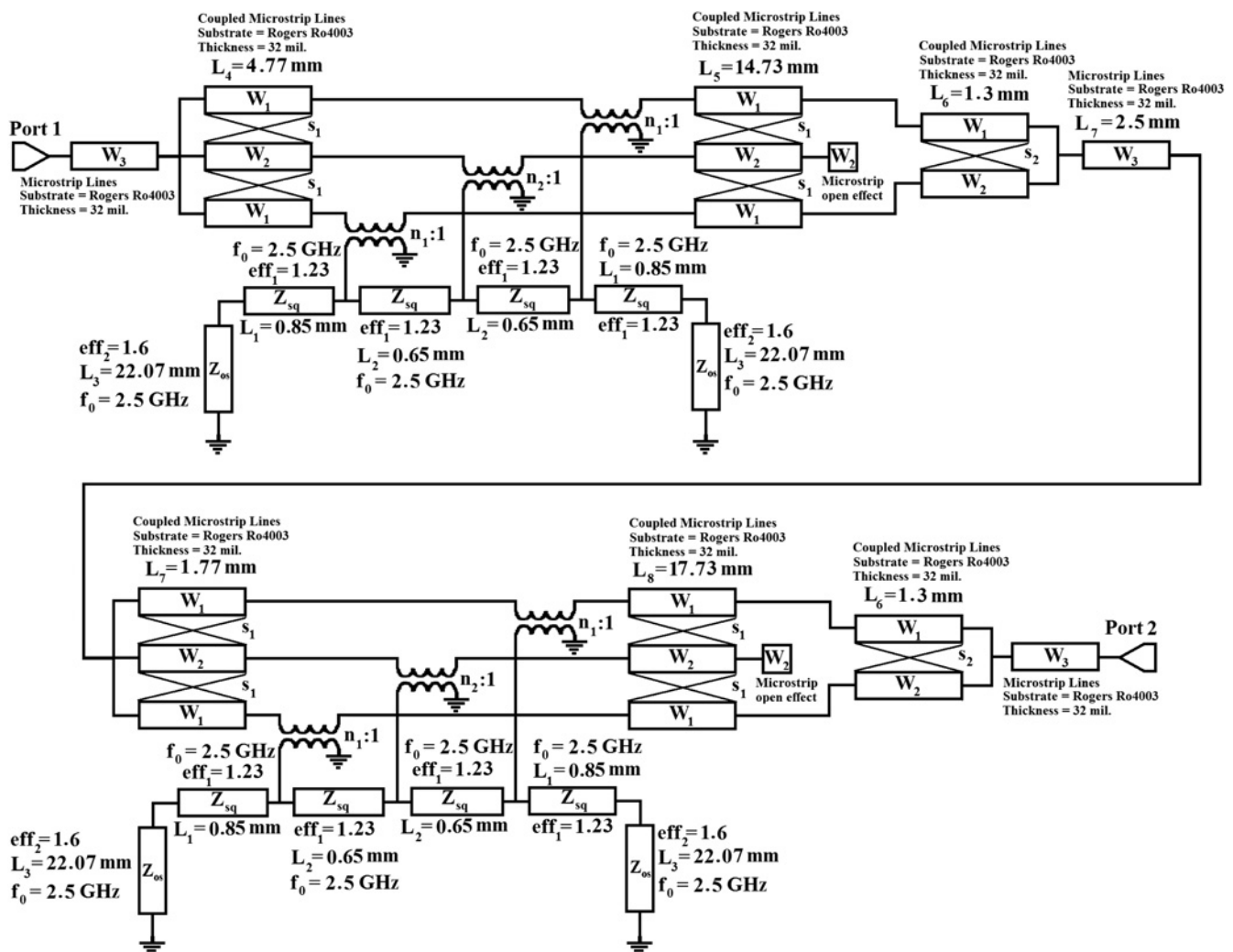


Fig. 7 Equivalent circuit model for the proposed SCSRR

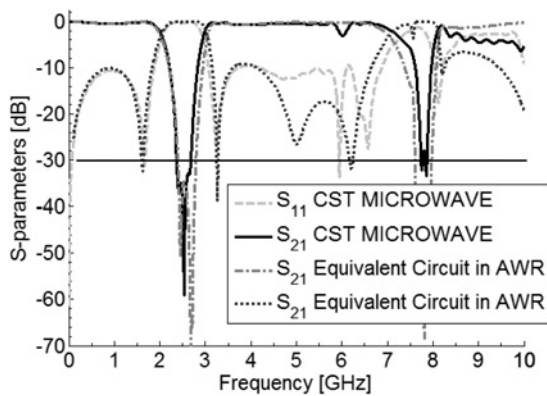


Fig. 8 Comparison of S -parameters between EM simulation and circuit simulation

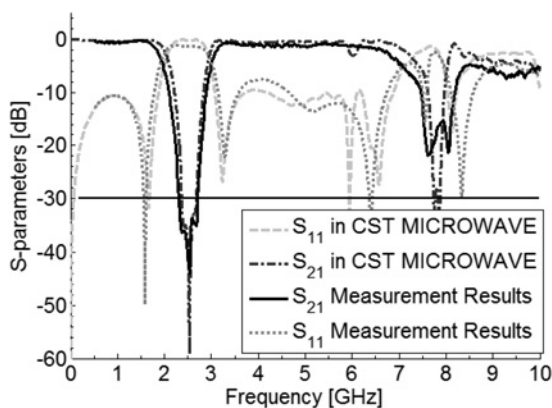


Fig. 9 Comparison of the simulated and the measured performances for the proposed filter

lower passbands are not changed after adding the LRs and this means that it still behaves as a regular microstrip line for the top and the bottom circuits, and the perturbation made by LRs in the microstrip lines is negligible.

6 Experimental results

Fig. 9 shows the S -parameter measurement and simulation results. The measurement is made with an HP 8722 vector network analyser, and shows that the magnitude of S_{21} is below -30 dB from 2.3 to 2.7 GHz and has -44 dB rejection around 2.53 GHz. The proposed filter exhibits good band-stop behaviour as predicted by the EM simulator. The small discrepancies can be attributed to fabrication tolerances and to the dissipative losses that were not taken into account in the simulation.

Going by the geometrical properties of this filter, the proposed SCSRR band-stop filter does not have an even harmonic response. In addition, except for the rejection frequency band, a flat and perfect matched passband is presented with very low insertion losses.

Finally, the results for this proposed filter are compared with other familiar metamaterials such as CSRR, and the filter in [19] is chosen as a benchmark. In [19], a band reject filter at 2.6 GHz is proposed by using four CSRR resonators on a Rogers RO3010 substrate with $\epsilon_r = 10$ and a thickness of 1.27 mm. The length of the filter excluding the access line for the connector is 28 mm. The filter in

[19] has a wide deep rejection band. Obviously, the size reduction over the proposed structure is as good as that in [19], with the overall filter length being about 45 mm, but a substrate with $\epsilon_r = 3.55$ and lower thickness (0.8218 mm) is used that decreases the overall effective permittivity. However, the present filter has a wide and low-loss passband after the rejection band. There is no second harmonic in the proposed structure. In contrast, in [19] the filter has ripples up to -5 dB and gives results only from 0–5 GHz, but if one considers Fig. 3a in [19] from the falling slope of the S_{21} near the 5-GHz frequency, it can be assumed the filter in [19] has a second harmonic.

7 Conclusion

This paper proposes a new SCSRR compact band-stop microstrip structure that has been successfully modelled and tested. The filter produces high rejection with sharp cutoffs in the stop band, and shows a completely flat and lossless passband. This behaviour can be interpreted as corresponding to a frequency band with negative value permittivity provided by the SCSRRs. It is potentially applicable to the wide variety of microwave circuits with monolithic microwave integrated circuit (MMIC), low temperature co-fired ceramic (LTCC) and micro-electro-mechanical systems (MEMS) technologies.

8 Acknowledgment

The authors thank Mr. Abbas Ghods and my Golbarg roommates for their assistance during this project.

9 References

- Shelkownikov, A., Suntheralingam, N., Budimir, D.: 'Novel SRR loaded waveguide bandstop filters'. IEEE Antennas and Propagation Society Int. Symp., 9–14 July 2006, pp. 4523–4526
- Naghshvarian-Jahromi, M., Tayarani, M.: 'Miniature planar UWB bandpass filters with circular slots in ground', *Progr. Electromagn. Res. Lett.*, 2008, **3**, pp. 87–93
- Scherer, A., Doll, T., Yablonovitch, E., Everitt, H.O., Higgins, J.A.: 'Guest editorial electromagnetic crystal structures, design, synthesis, and applications', *J. Lightwave Technol.*, 1999, **17**, pp. 1928–1930
- Smith, D.R., Padilla, W.J., Vier, D.C., Nemat-Nasser, S.C., Schultz, S.: 'Composite medium with simultaneously negative permeability and permittivity', *Phys. Rev. Lett.*, 2000, **84**, pp. 4184–4187
- Joannopoulos, J.D., Meade, R.D., Winn, J.N.: 'Photonic crystals: molding the flow of light' (Princeton University Press, Princeton, NJ, 1995)
- Radisic, V., Qian, Y., Coccioli, R., Itoh, T.: 'Novel 2-D photonic bandgap structure for microstrip lines', *IEEE Microw. Guided Wave Lett.*, 1998, **8**, pp. 69–71
- Laso, M.A.G., Lopetegi, T., Erro, M.J., Benito, D., Garde, M.J., Sorolla, M.: 'Multiple-frequency-tuned photonic bandgap microstrip structures', *IEEE Microw. Guided Wave Lett.*, 2000, **10**, pp. 220–222
- Yang, F.R., Ma, K.P., Qian, Y., Itoh, T.: 'A uniplanar compact photonic-bandgap (UC-PBG) structure and its applications for microwave circuits', *IEEE Trans. Microw. Theory Tech.*, 1999, **47**, pp. 1509–1514
- Yang, F.R., Coccioli, R., Qian, Y., Itoh, T.: 'Planar PBG structures: basic properties and applications', *IEICE Trans. Electron.*, 2000, **E83-C**, (5), pp. 687–696
- Pendry, J.B., Holden, A.J., Robbins, D.J., Stewart, W.J.: 'Magnetism from conductors and enhanced nonlinear phenomena', *IEEE Trans. Microw. Theory Tech.*, 1999, **47**, pp. 2075–2084
- Falcone, F., Martín, F., Bonache, J., Martel, J., Marqués, R., Lopetegi, T., Laso, M.A.G., Sorolla, M.: 'Implementation of negative- ϵ structures in microstrip technology'. Proc. 28th Int. Conf. Infrared Millimeter Waves (IRMMW'03), Shiga, Japan, September/October 2003
- Park, A.D., Kim, J.-S., Kim, C.-S., Qian, J., Itoh, Y.T.: 'A design of the low-pass filter using the novel microstrip defected ground structure', *IEEE Trans. Microw. Theory Tech.*, 2001, **49**, pp. 86–93

- 13 Karim, M.F., Liu, A.-Q., Alphones, A., Zhang, X.J., Yu, A.B.: 'CPW band-stop filter using unloaded and loaded EBG structures', *IEE Proc. Microw. Antennas Propag.*, 2005, **152**, pp. 434–440
- 14 Görür, A., Karpuz, C.: 'Resonance characteristics of capacitively loaded CPW open-loop resonators', *Microw. Opt. Technol. Lett.*, 2003, **38**, pp. 298–300
- 15 Singh, R.B., Weller, T.M., Smith, M.C., Culver, J.W.: 'Capacitively loaded CPW shunt stub notch filters', *Microw. Opt. Technol. Lett.*, 2003, **36**, pp. 292–295
- 16 Hamad, E.K.I., Safwat, A.M.E., Omar, A.S.: 'Controlled capacitance and inductance behaviour of L-shaped defected ground structure for coplanar waveguide', *IEE Proc. Microw. Antennas Propag.*, 2005, **152**, pp. 299–304
- 17 Kim, J.P., Park, W.S.: 'Novel configurations of planar multilayer magic-T using microstrip-slotline transitions', *IEEE Trans. Microw. Theory Tech.*, 2002, **50**, (7), pp. 1683–1688
- 18 Yen, K.U., Wollack, E.J., Papapolymerou, J., Laskar, J.: 'A broadband planar magic-T using microstrip-slotline transitions', *IEEE Trans. Microw. Theory Tech.*, 2008, **50**, (1), pp. 172–178
- 19 Falcone, F., Lopetegi, T., Baena, J.D., Marqués, R., Martín, F., Sorolla, M.: 'Effective negative- ϵ stopband microstrip lines based on complementary split ring resonators', *IEEE Microw. Wirel. Compon. Lett.*, 2004, **14**, (6), pp. 280–282
- 20 Mao, S.-G., Chen, S.-L., Huang, C.-W.: 'Effective electromagnetic parameters of novel distributed left-handed microstrip lines', *IEEE Trans. Microw. Theory Tech.*, 2005, **53**, (4), pp. 1515–1521
- 21 Nicholson, A.M., Ross, G.F.: 'Measurements of the intrinsic properties of materials by time-domain techniques', *IEEE Trans. Instrum. Meas.*, 1970, **19**, (4), pp. 377–382
- 22 Weir, W.B.: 'Automatic measurements of complex dielectric constant and permeability at microwave frequencies', *Proc. IEEE*, 1974, **62**, (1), pp. 33–36
- 23 Zhang, J., Cui, B., Lin, S., Sun, X.-W.: 'Sharp-rejection low-pass filter with controllable transmission zero using complementary split ring resonators (CSRRLs)', *Progr. Electromagn. Res.*, 2007, **PIER 69**, pp. 219–226
- 24 Dimmock, J.O.: 'Losses in left-handed materials', *Opt. Express*, 2003, **11**, pp. 2397–2402
- 25 Ali, A., Hu, Z.: 'Negative permittivity meta-material microstrip binomial low-pass filter with sharper cut-off and reduced size', *IET Microw. Antennas Propag.*, 2008, **2**, (1), pp. 15–18
- 26 Deschamps, G.A.: 'Impedance properties of complementary multiterminal planar structures', *IRE Trans. Antennas Propagat.*, 1959, **AP-7**, pp. 371–378
- 27 Gupta, K.C., Garg, R., Bahl, I., Bhartia, P.: 'Microstrip lines and slotlines' (Artech House Inc, Boston, London, 1996, 2nd edn.)
- 28 CST Microwave Studio, Computer Simulation Technology 2009